CENTRIFUGE CAPILLARY PRESSURE DATA INTERPRETATION: GRAVITY DEGRADATION ASPECT CONSIDERATION

Zhigang Andy CHEN *and* **Douglas W. RUTH**

University of Manitoba, Winnipeg, MB, CANADA R3T 5V6

ABSTRACT

The gravity degradation phenomenon at low speeds (less than 500 rpm *when initiating centrifuge capillary pressure experiments) has been identified as one of the problems for high permeability and porosity sandstone core samples. For these samples, the gravitational acceleration distorts the horizontal centrifugal force field distribution inside the core plug, thereby leading to inaccurate interpretation of capillary pressure information in the high saturation zone (near the threshold pressure). On the basis of a three dimentional centrifuge theory characterizing such an effect, this paper investigates the numerical technique which allows the gravity acceleration at low speed to be included for traditional Beckman centrifuges. Several capillary pressure versus saturation relationships are used to conduct parameter estimations. Tested examples show that the implicit parameter estimation algorithm based on the three-dimensional model of centrifuge experiments can provide more accurate information in the high saturation zone.*

INTRODUCTION

The centrifuge method of determining capillary pressure curves and rock saturations was initially developed by Hassler and Brunner in 1945. Since then it has found wide application in many aspects of core analysis. However, two major problems, associated with fundamental assumptions, still complicate the proper application of the centrifuge technique in obtaining accurate data. These problems are the radial effect, due to core width, and the gravity effect, due to low initial ramp-up speeds. Christiansen and Cerise (1988) and Christiansen (1992) realized the possible errors of the one dimensional model and developed a two-dimensional model to account for the radial centrifugal field distribution. They found systematic errors due to this effect. Ayappa *et al.* (1989) also discussed models for arbitrary-shaped core samples and they derived the relevant governing equations. Recently, Forbes et al (1993, 1994) re-evaluated this problem and provided a semi-analytical solution to quantitatively account for the radial effect in practical applications.

The gravitation problem was recognized initially by Ruth and Chen (1992) for the traditional rotor design of Beckman centrifuges. Rotors that come with these centrifuges contail a horizontal head and the sample is exposed to a gravity effect at low speeds. Core plugs in the rotor are usually spun in a horizontal plane and the centrifugal force is also assumed to be acting horizontally (perpendicular to the vertical rotational axis). In reality, because of the gravitational acceleration of the earth, where the rotating centrifugal field and the earth's gravitational field are at right angles, the true force acting on a fluid particle inside a core plug will be "*dragged down*", creating an inclined acceleration field. Thus, gravitational acceleration leads to a total acceleration field that is not purely centrifugal. This effect is referred to as "gravity degradation " in the present study. It is generally postulated that gravity degradation occurs in high permeability and porosity core sample experiments where low angular speeds are used initially. Chen and Ruth (1993b) worked out a 3D theory to characterize this problem, and with synthesized data they found a huge discrepancy in production curves at high saturations for most brine-air, high-permeability sandstone experiments. However, they did not quantify how this effect is reflected in capillary pressure curves, which is the most important topic in centerifuge data interpretations. This paper discusses the effect of the gravity degradation on the interpreted capillary pressure curve given a set of production data (mean saturations versus rotational speeds).

GRAVITY DEGRADATION THEORY

Conventional Beckman centrifuges have fixed, horizontal rotors. When describing a rotating fluid in hydrostatic equilibrium (Figure 1), we can start from Newton's second law in a Cartesian coordinate system and derive the following equation

$$dP = \rho\omega^2(xdx + ydy) - \rho g dz \tag{1}$$

where P denotes the pressure of a particle of a fluid at any location, dP the differential pressure, ω the angular speed, ρ the fluid density, g the gravational acceleration and z the vertical coordinate (positive upward).

Integrating this equation results in

$$P = \frac{1}{2}\rho\omega^2(x^2 + y^2) - \rho g z + C \tag{2}$$

Defining a reference point will allow the determination of C in the above equation. According to Eq. 2, the rotating centrifuge force field with earth gravity effect can be visualized as a paraboloid of revolution. In order to link capillary pressure fields and saturations under different angular speeds for the core sample, it has been an effective tool to introduce the concept of **equipotential surfaces** to describe the iso-potential contour distribution of fluid pairs inside the core sample. Ayappa *et al.* (1989) were the first to use this concept to characteize centrifugal force field distributions. Let $A(r_0)$ be an equipotential surface inside the core plug, where r_0 is the rotation distance from a reference point of an intersecting process of the rotating paraboloid with a cylinder—the core plug cylinder. For such equipotential surfaces, there should be $\int A(r_0)dr_0 \equiv \pi R^2(r_2 - r_1) = V$, where V represents the core plug volume, r_1, r_2 and R are the geometric parameters of the core plug, and

$$\overline{S}_w = \frac{1}{V}\int_{r_{0min}}^{r_{0max}} S_w(P_c)A(r_0)dr_0 \tag{3}$$

where r_{0min} and r_{0max} are the two limiting boundaries.

An equipressure surface always implies that $dP = 0$, which from Eq. 1, expressed in cylindrical rather than Cartesian coordinates, leads to

$$\rho\omega^2 r dr = \rho g dz \tag{4}$$

and

$$\frac{1}{2}\omega^2(r^2 - r_0^2) = g(z - z_0) \tag{5}$$

where (r, z) and (r_0, z_0) are any two points on the equipressure surface. Eq.5 describes clearly the three dimensional force field distribution: not only a radial centrifugal field, but a vertical gravitational acceleration is acting. Because of the vertically acting gravitational acceleration, the centrifugal field is dragged down, leading to the creation of a net force with an inclined angle of α relative to the horizontal. As the rotation speed ω increases, the effect of g becomes neglegible, that is $\alpha = 0$, and the capillary pressure is counterbalanced by a pure, horizontal centrifugal force. When $\omega = 0$, $\alpha \to 90°$, and the capillary pressure is related only to the vertical gravitational acceleration field. When initiating an experiment with a centrifuge, there is always a combined distribution of both horizontal centrifugal and vertical gravitational fields, and the inclination of the distribution is strongly dependent on the rotation speeds used during the experiment. At low speed stages for an experimental run, gravitational acceleration plays a significant role in *distorting* the pressure distribution.

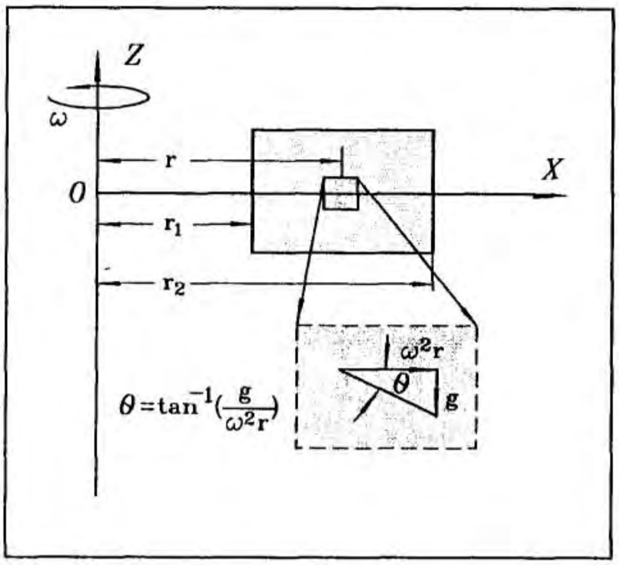

Figure 1. Gravity Degradation Effect

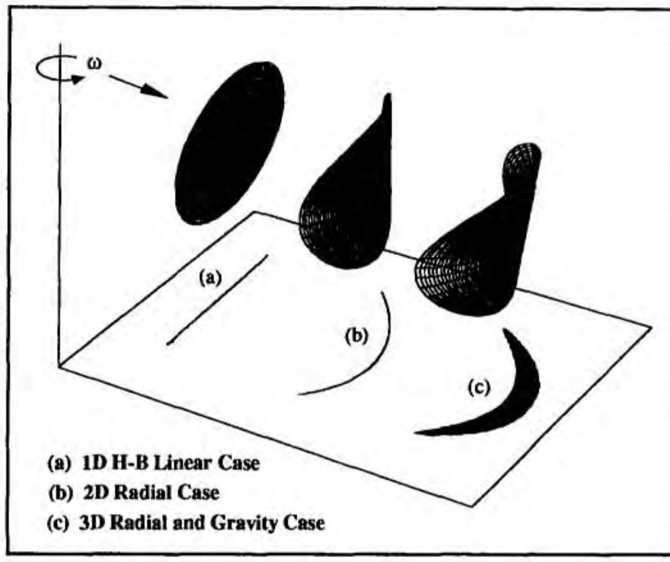

Fgiure 2. Different Equipotential Surfaces

Now let us define (r, z) as any point inside the core plug, and select (r_0, z_0) at the top line of the core sample plug. We then have $z_0 = R$. This condition is imposed because we assume that the initial pressure distribution in the cross-section of the core sample is hydrostatic. Accordingly, if we define $C_g = \frac{2g}{\omega^2}$, Eq.5 is re-written as

$$r^2 = x^2 + y^2 = r_0^2 + C_g(z - R) \tag{6}$$

or

$$x^2 = r_0^2 - y^2 + C_g(z - R) \tag{7}$$

It follows that $x = f(y, z)$ for the equipotential surface that passes through the point $r = r_0$, $z = z_0$. Therefore we can write

$$A(r_0) = \int\int F(x, y, z)\ dz\ dy \tag{8}$$

where $F(x, y, z) = \sqrt{1 + f_y^2 + f_z^2}$, and $f_y = \frac{\partial x}{\partial y}$, $f_z = \frac{\partial x}{\partial z}$ (Thomas, 1960).

Equipotential Surfaces. If r_0 is used (for convenience, we use x instead of r_0 in a Cartesian system) as the reference linear distance from the axis of rotation to locations on the top line of the core plug cylinder, then when performing the integration of Eq.3, one has to separate the integrand for different ranges of r_0 in order to account for the distribution of equipotential surfaces inside the core plug. Here

r_0 is equivalent to the r in Christiansen's case. The range of r_0 is divided into several zones, depending on different combinations of the parameters involved in the problem. Generally, when $C_g \leq 2R$, there are five zones, with

$$r_{0min} = r_{inlet}$$

and

$$r_{0max} = \sqrt{R^2 + r_{outlet}^2 + RC_g + \frac{C_g^2}{4}}$$

where r_{inlet} corresponds to the *first touch* of the "paraboloid" with the core plug "cylinder", and r_{outlet} the *last touch* of the "paraboloid" with the "cylinder". When $C_g \geq 2R$, only three zones are observed, and $r_{0min} = r_{inlet}$ and $r_{0max} = \sqrt{r_{outlet}^2 + 2RC_g}$ for this situation. Figure 2 gives a comparison of equipotential surfaces for various cases with synthesized data: 1D Hassler-Brunner case, 2D Christiansen's radial concern, and 3D theory including both the radial and the gravity effects. The determination of the integral boundaries and the distinction of all those zones are discussed in detail elsewhere (Chen and Ruth, 1993b).

Capillary Pressure Calculations. In order to obtain capillary pressure curves, we need to define a reference capillary pressure, which is usually chosen at a boundary. For the problem under study, it has been postulated that the reference maximum capillary pressure is expressed as

$$P_c = \frac{1}{2}\Delta\rho\omega^2(r_{0max}^2 - r_{inlet}^2) \tag{9}$$

if the zero-capillary pressure is assumed to take place at the two tangent points located at the edge of the outside endface ($x = r_{outlet}$, $y = \pm\sqrt{R^2 - \frac{C_g^2}{4}}$, $z = -\frac{C_g}{2}$). When C_g is exceptionally large ($C_g > 2R$), the zero P_c boundary condition takes place at the bottom point of the outside endface of the core plug cylinder. Again in this problem, r_{0max}, the maximum radius required for a zero-capillary pressure boundary, can be calculated as: when $C_g \leq 2R$, $r_{0max} = \sqrt{r_{outlet}^2 + R^2 + RC_g + \frac{C_g^2}{4}}$, and when $C_g \geq 2R$, $r_{0max} = \sqrt{r_{outlet}^2 + 2RC_g}$.

Thus, capillary pressure at any point inside the core sample plug can be calculated using the following equation

$$P_c(r,z) = \frac{1}{2}\Delta\rho\omega^2\left(r_{0max}^2 - r^2 - C_g(R-z)\right) \tag{10}$$

For the purpose of performing the integration in Eq.3, the capillary pressure at any point on the top line of the core cylinder is

$$P_c(r_0) = \frac{1}{2}\Delta\rho\omega^2\left(r_{0max}^2 - r_0^2\right). \tag{11}$$

A quantitative study on the potential effect of the gravity degradation on production performance has been reported elsewhere (Chen and Ruth, 1993b). The results for synthesized data sets show that for ramp-up speeds of centrifuge experiments below *500 rpm*, there is a major distortion on production curves caused by gravity degradation, especially for those high permeability/porosity sandstone runs that are usually initiated with an angular speed of *200 rpm*.

Physically, when we explain what the gravity effect is all about, we can combine this question with the radial effect. Traditionally, Hassler and Brunner's simplified one-dimension case considers a constant linear centrifugal field (Forbes, Chen and Ruth, 1994b) with a straight line projection of the equipotential surface into a horizontal plane, as shown in Figure 2. The radial effect is accounted for if core width is considered, and the equipotential surface is distorted by this effect. Phenomenologically, this distortion leads to a larger area of the equipotential surface than that of the non-distorted Hassler-Brunner equipotential surface, which looks like a vertical disk. In other words, $A_{radial}(r_0) \geq A_{HB}(r_0)$ in practice due to the core width consideration. When we go to the three-dimension case with gravitational acceleration included, ths distortion of the equipotential surface becomes even worse, and the area of the 3D distorted surface is larger than that of the 2D radially distorted surface. Therefore, with the 3D centrifuge theory which includes all of the effects of centrifuge experiment physics, we can conclude that $A_{HB}(r_0) \leq A_{radial}(r_0) \leq A_{radial+gravity}(r_0)$. This observation can be supported by Figure 2, which shows the calculated result for the different cases under consideration.

GRAVITY EFFECT ON CAPILLARY PRESSURE CURVES

In this section, we will address how gravitational acceleration affects capillary pressure cuvres. This involves some details of data interpretation techniques for centrifuge capillary pressure curve reduction. The previous study (Chen and Ruth, 1993b) investigated the effect of gravity degradation on production performance of centrifuge runs. As discussed by many people (Ruth and Wong, 1990; Ruth and Chen, 1992; Chen and Ruth, 1993a; Forbes, Chen and Ruth, 1994b), generating a production history from a capillary pressure relationship is a direct process, which can usually give a unique solution, while interpreting a centrifuge capillary pressure curve from raw experimental data (production history) is an inverse process. This inverse process involves implicit methods. As suggested by Ayappa *et al.* (1989), Eq.3 is a Volterra integral equation of the first kind, and is known to be strongly numerically unstable. It is very difficult if not impossible to find its explicit analytical solution because of its three dimensional complexity. However, we can use implicit methods or parameter estimation techniques, assuming some explicit capillary pressure functional models, to quantify the error introduced in conventional one dimensional or two dimensional analyses (neglecting gravity effects). Basically, people follow two major ways in assuming capillary pressure functional models: simplistic model representations and spline functions (Nordtvedt and Kolltveit, 1991). Our purpose here is to test the gravity effect for parameter estimations, and we have chosen some simplistic models to characterize capillary pressure relationships.

Capillary Pressure Relationships. Numerous capillary pressure functional relationships have been proposed for numerical simulations. These relationships include: (1) Bentsen's log- and power- forms (Bentsen and Anli, 1977; Golaz and Bentsen, 1980), $P_c = P_d + a\ln(\frac{S_w - S_{wr}}{1 - S_{wr}})$, and $P_c = P_d + a(\frac{S_w - S_{wr}}{1 - S_{wr}})^b$, where P_d is the threshold pressure, S_{wr} the irreducible connate water saturation, and a, and b are parameters to be estimated; (2) Corey's (1954), $P_c = P_d(\frac{S_w - S_{wr}}{1 - S_{wr}})^{-\frac{1}{\lambda}}$; (3) Thomeer's (1960), $\frac{S_g}{S_{b\infty}} = \exp(-\frac{F_g}{\log P_c/P_d})$; (4) Chen *et al.*'s (1992), $\frac{S_w - S_{wr}}{1 - S_{wr}} = \frac{1}{1 + a(P_c - P_d)^b}$; (5) van Domselaar's (1984), $S_w = S_{wr} + (1 - S_{wr})\frac{P_d}{P_c}$; (6) those suggested by Forbes (1993), $\frac{S_w - S_{wr}}{1 - S_{wr}} = \ln(1 + c\frac{P_d}{P_c})$, and $\frac{S_w - S_{wr}}{1 - S_{wr}} = \sum_i a_i(\frac{P_c}{P_d})^i$.

Hirasaki and Rohan (1993) also suggested the use of lognormal and bimodal lognormal relationships. All these functions can be used to test the effect of gravitational degradation on capillary pressure curves. It is difficult to determine the superiorty of any certain expression for particular applications in centrifuge capillary pressure interpretation techniques. However, as far as this particular problem is concerned, we recommend the use of expressions that give better flexibility in representing the whole curve, including a possible reversal of curvature near $S_w \to 100\%$.

Synthesized Dataset. In order to examine and quantify the effect of gravity degradation on capillary pressure curves, many synthesized datasets have been constructed. Two data examples are shown in this paper to illustrate the problem. Bentsen's log and Chen *et al.*'s expressions are used to reflect the effect of the gravity degradation factor in the interpreted capillary pressure. Concerning our particular physical problem, we assume that the threshold pressure $P_d = 0$, and for Bentsen's expression, a is

0.50 *psi*. We are looking at typical values of high permeability ($k > 700$ *md*) and porosity ($\phi > 20\%$) sandstone sample experiments, including unconsolidated tar sand core samples. The density difference value is assumed to be 1.01 g/cm^3, representing a typical air-brine experiment. As used in Christiansen's paper (1992), the irreducible connate water saturation S_{wr} is selected as 0.2. The rotational speed (in *rpm*) dataset includes 50, 100, 150, 200, 300, 400, 500, 600, 800, and 1000 (for high permeability and porosity samples, the *rpm* schedule should include speeds from 150 to 500 *rpm*). The rotor and core plug system is assumed to be characterized by $r_{inlet} = 6.06\ cm$, $r_{outlet} = 8.6\ cm$, and $R = 1.27\ cm$. This corresponds to a 1.0 inch long and 1.0 inch diameter core sample, mounted in a rotor with an outer rotation distance of 8.6 *cm*. These numbers are typical for a Beckman centrifuge.

For capillary pressure calculations, we have used

$$P_c(x, y, z) = 0.7953473 \times 10^{-7}\ \Delta\rho(rpm)^2(r_{0max}^2 - x^2 - y^2 - C_g(R - z)) \tag{12}$$

where r_{0max} is defined in the previous section.

SCA Survey Data. We have also tried to include some real data to evaluate this problem. Two SCA survey datasets were selceted to test this effect. They are the core samples numbered **EF3** and **FA4**. **EF3** has a permeability of 627 md, and $\phi = 23.20\%$. The density difference of the fluid system is 1.011 $\frac{g}{cm^3}$, and the low rotational speed of the experiment ranges from 190 *rpm* to 600 *rpm*. The properties of **FA4** include 754 md and 23.00% for permeability and porosity respectively. Again the fluid system had a density difference of 1.011 $\frac{g}{cm^3}$, but the low speed range for this test was from 300 *rpm* to 680 *rpm*. The experiments for the samples were made with a **Beckman L8-55 M/P** centrifuge, with $r_{outlet} = 8.6\ cm$. The other details reported about the core samples and the experiments can be found in The Society of Core Analysts survey.

RESULTS AND DISCUSSION

For the Hassler-Brunner one dimensional analysis, the capillary pressure at the whole inlet endface is assumed to have the same value, that is P_{c1} is uniform everywhere on the inlet endface. Christiansen introduced a P_{c1} which occurs at the vertical center line (from the top to the bottom) of the inlet endface. For the three dimensional consideration, the P_{c1} is located at the top point of the inlet endface. Therefore, we have chosen the P_{c1} from Eq. 12 as the reference value which makes the most sense for the practical situations. As found by the previous study (Chen and Ruth, 1993b), the three dimensional values are always located above the one and two dimensional values, while Hassler-Brunner's one dimensional values are always less then the others. When the rotation speed exceeds 500 *rpm*, the three dimensional values converge on Christiansen's two dimensional values, because above this speed the effect of C_g vanishes and the three dimensional model is identical to Christiansen's theory. Christiansen's model does not include the gravity effect and from the curves it can be seen that his lines are basically equivalent to Hassler-Brunner's solutions at low speed. Neither Ayappa *et al* (1989) nor Christiansen (1992) studied data interpretation in the low speed zone in their studies.

Eq.3 was used to test the significance of the gravitational acceleration. The Gauss-Legendre algorithm (Maron, 1982) was used to numerically evaluate the triple integral. Grid refining tests were carried out using 50 points in the Gauss-Legendre algorithm and sufficient precision was obtained (Stroud and Secrest, 1966). All computations were run using double precision on a SunFortran system.

Figures 3 and 4 give the results for simulated datasets with the two models. Lines and filled circles are to distinguish the difference of the curves obtained with different theoreties. "*Christiansen*" means the curve obtained with the 2D theory developed by Christiansen (1992). Each example used 12 points in data column covering primarily the low speed range. A systematic discrepancy is found in both interpretations. The trend for gravity degradation consideration is similar to that introduced by the radial effect to modify the traditional one-dimensional Hassler-Brunner case, that is, at the high saturation zone of capillary pressures curves, the curve recovered with the gravity-included theory is always higher than the one with Christiansen's 2D model which considers the radial effect only. This result seems to be reasonable, because when generating the mean saturation history, the 3D theory gives lower values than the 2D model at low speeds. The mean saturations generated with the 3D theory are recoverable using numerical simulation techniques, while when using Christiansen's 2D model to convert the generated mean into a capillary pressure, the recovered curve always seems to be lower than the original curve. This observation is basically similar to the radial effect problem. We have used several other models trying to quantity this discrepancy, and have found that the difference in the interpreted capillary pressures ranges from 1 to 5 saturation percent, depending on individual cases. The information provided in these two figures is that the capillary pressure curve obtained with the 3D theory, which considers both the radial and the gravity effects, is different from the one interpreted from Christiansen's 2D theory, which considers the radial effect only.

However, when interpreting these curves using implicit numerical simulation algorithms, we identified a new problem. Beacuse the gravity degradation occurs at low speeds, only the section of the curve at high saturation is affected. On the other hand, simplistic capillary pressure functions, which have to be pre-assumed, provide few model parameters to be estimated in order to achieve an optimized fitting of production performance (mean saturations). The outcome of this difficulty is that the recovered capillary pressure curves with implicit methods might have an overall shift. As an example in Figure 3, the recovered capillary pressure curve with Christiansen's 2D theory (dash-dotted-dotted) has moved generally downward, but this seems to include high rotational speeds. In other words, the spread of the gravity degradation effect can be out of the mentioned low speed range ($\leq$ 500 *rpm*) with implicit data reduction algorithms. Sometimes, the interpreted capillary pressure curve can be actually **"forced"** to bend. This can be observed by the second example in Figure 4, where Chen *et al.*'s reversal cruvature model is used to test the effect. It can be seen that the 3D theory again recovers the original capillary pressure curve, while when converting the 3D generated mean saturation data with Christiansen's 2D model, we obtained a forced-to-bend curve: the high saturation section is below the original curve, while the medium-low saturation section (between 20% to 40%) is above the original curve. We tried to use other models with only a few adjustable model parameters to recover capillary pressure curves, but the results were not very successful.

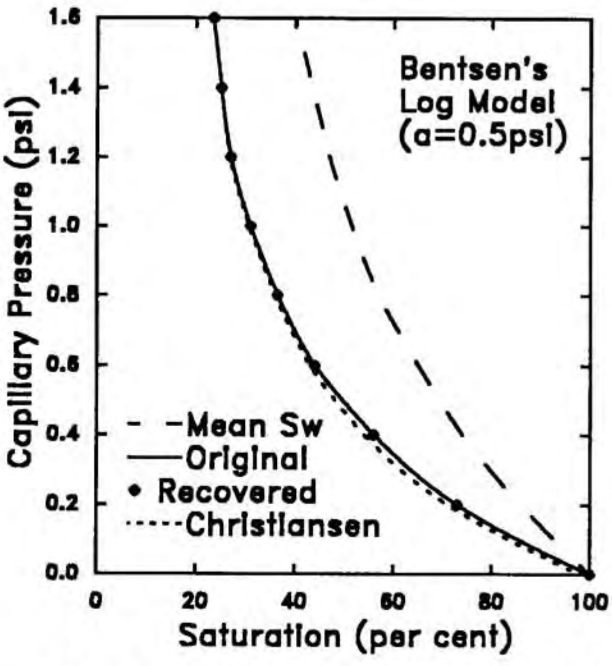

Figure 3. Bentsen's Log Model

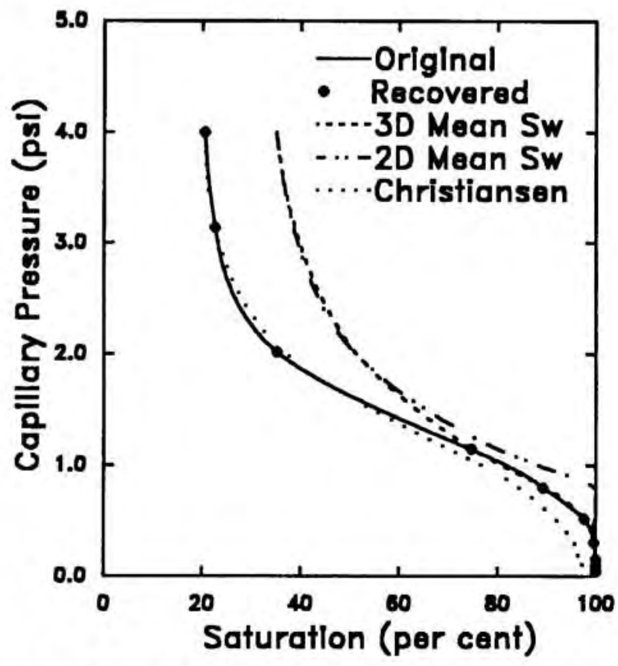

Figure 4. Chen *et al.*'s Reversal Curvature Model

This shows the limitation of simplistic capillary pressure functions in implicit methods for centrifuge data reduction. We expect more complicated forms of such functions to provide better curve fits, especially the B-splines suggested by Nordtvedt and Kolltveit (1991). However, this method involves complicated numerical algorithms. It should be pointed out that this new problem arises due to the limitation of the implicit interpretation method itself, which does not really alter the *de facto* gravity degradation effect that we have identified above. Because of the numerical difficulty, we have suggested an alternate remedy to overcome the porblem, that is, adopting pivoted rotor heads in centrifuges to minimize the gravity effect inside core samples (Chen and Ruth, 1994).

In reality, we do not expect gravity degradation to play a major role in most centrifuge experiments, unless high permeability and porosity core samples are tested. We have found in the SCA centrifuge capillary pressure survey that most experimental datasets were collected for angular speeds higher than 500 *rpm*. Figures 5 and 6 provide two examples for these raw experimental data. Each example contains 15 data points covering both low and high speeds. Again we have used the reversal-curvature function, and have recovered two capillary pressures curves for each sample, with the curves converted by the 3D theory providing a different interpretation. When we inspected many of the centrifuge capillary pressure curves (we assume that those curves were all obtained with conventional interpretation techniques without considering the gravity effect) from The SCA survey report (Yuan, 1993), there was either a shortage of high-saturation data, or much lower saturation values at low initial rotational speeds, as can be seen in Figure 5. Figure 6 gives another example, but the difference is not pronounced. Note

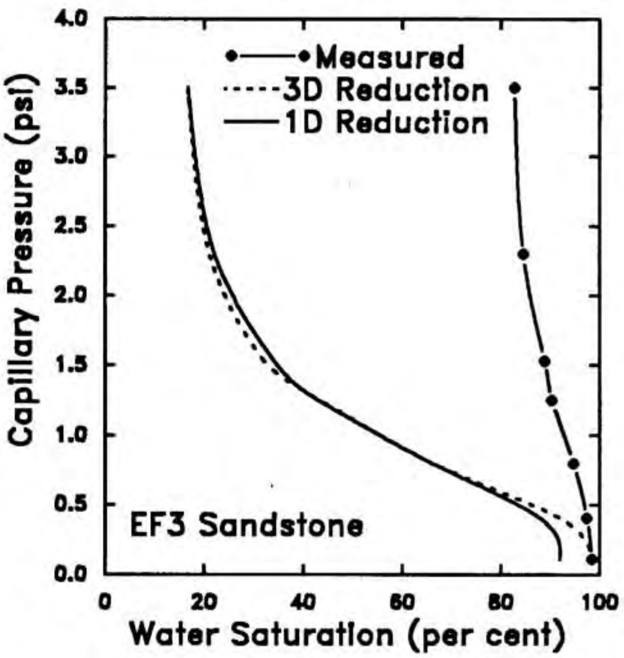

Figure 5. SCA Survey Data: EF3

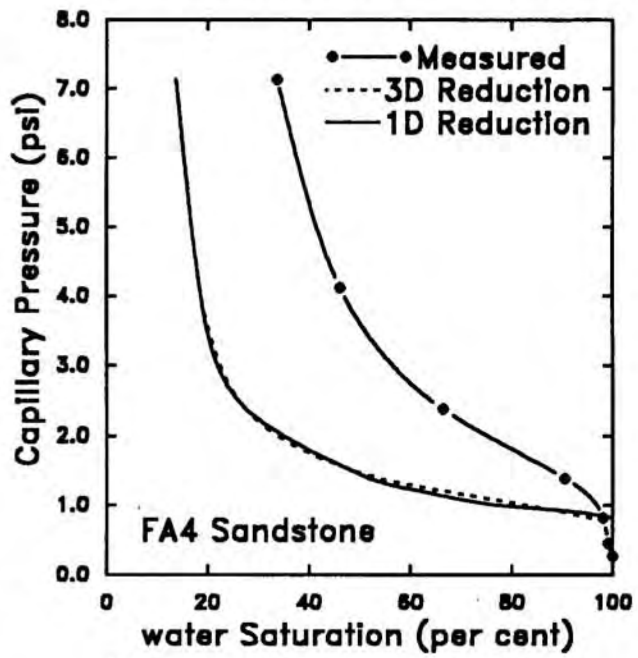

Figure 6. SCA Survey Data: FA4

that we are describing the gravity effect theoretically. Experimental verification of this phenomenon remains to be achieved. Other potential applications include similar centrifuge capillary pressure measurements in soil science, where high permeability and porosity values are expected and centrifuge runs are also subject to low ramp-up speeds (Klute, 1986).

CONCLUSION

- A three dimensional theory is used to convert centrifuge experimental data into capillary pressure curves considering all major physical problems, especially gravity degradation considerations. Numerical simulation techniques developed based on this theory show that the 3D model provides a better description of capillary pressure curves from centrifuge experiments in the high saturation zones (low initial angular speeds);

- There is a systematic discrepancy between capillary pressure curves obtained from the 3D theory and from Christiansen's 2D model, at the threshold zone of capillary curves, with the 3D curves generally higher than the traditional curves from either 1D Hassler-Brunner's or the 2D Christiansen's centrifuge theories.
- Implicit data interpretation techniques have to be used to recover the true capillary curve. Capillary pressure functional relationships involved in parameter estimation, should include sufficient adjustable parameters to allow optimized production curve fitting.

Acknowledgement The authors would like to thank ESSO Resources and NSERC for financial support for this project.

Nomenclature

$A(r_0)$	the equipotential surface area, cm^2
C_g	the characteristic factor, $C_g = \frac{2g}{\omega^2}$, cm
g	gravity acceleration, $\frac{cm}{sec^2}$
P_c	capillary pressure
P_{c1}	maxmium capillary pressure at the reference point r_{inlet}
P_d	Threshold capillary pressure
R	the radius of core cylinder plug, cm
r	rotation radius, cm
r_0	reference rotation radius, cm
r_{inlet}	the inner endface radius of rotation, cm
r_{outlet}	the bottom endface radius of rotation, cm
r_{0max}	the maxmium reference rotation radius, cm
r_{0min}	the minimum reference rotation radius, cm
S_w	wetting phase saturation
S_{wr}	irreducible connate wetting phase saturation
$\overline{S}_w$	mean wetting phase saturation
V	the volume of core sample plug, cm^3
x	variable
y	variable
z	variable
z_0	variable corresponding to r_0
$\Delta\rho$	density difference of fluid pairs
ω	angular rotation speed, $(rpm \times \frac{2\pi}{60}, \frac{1}{sec})$

References

Ayappa, K.G., Davis, H.T., Davis, E.A. and Gordon, J., 1989, Capillary pressure: Centrifuge method revised: *AIChE Journal*, **35**, 365-372.

Bentsen, R.G. and Anli, J., 1977, Using parameter estimation techniques to convert centrifuge data into a capillary-pressure curve: *Soc. Pet. Engr. Jour.*, **17**, 57-64.

Chen, Z., Liu, H.Q. and Yao, J., 1992, New capillary pressure models for parameter estimation to interpret centrifuge data: *SPE paper 24045* presented at 1992 SPE Western Regional Meeting, Bakersfield, CA, March 30-April 1.

Chen, Z.A. and Ruth, D.W., 1993a, Centrifuge capillary pressure data reduction with modified Forbes method: *Journal of Petroleum Science and Engineering*, **9**, 303-312.

Chen, Z.A. and Ruth, D.W., 1993b (submitted), The gravity degradation effect on low-speed centrifuge capillary pressure data: *AIChE Journal* (accepted for publication and in press).

Chen, Z.A. and Ruth, D.W., 1994, Centrifugal analysis of pivoted rotor systems for capillary pressure measurements: *CIM paper 94-77* presented at The 45th Annual Technical Meeting of The Petroleum Society of CIM, Calgary, Alberta, June 12-15.

Christiansen, R.L. and Cerise, K.S., 1988, Capillary pressure: reduction of centrifuge data: *SPE Unsolicited paper 19024*.

Christiansen, R.L., 1992, Geometric concerns for accurate measurement of capillary pressure relationships with centrifuge methods: *SPE Formation Evaluation*, **7**, 311-314.

Corey, A.T., 1954. The interrelation between gas and oil relative permeabilities. *Producers Monthly*, Nov. 38-41.

Forbes, P., 1993, Analysis techniques for centrifuge data: Part 1. Review of data analysis procedures. *The Centrifuge Capillary Pressure Workshop* at The Society of Core Analysts 1993 Annual Technical Conference, Houston, Texas, August 9-11.

Forbes, P., Ruth, D.W. and Chen, Z., 1994a, Discussion of geometric concern for accurate measurement of capillary pressure relationships with centrifuge methods. *SPE Fromation Evaluation*, **9**, 79-80.

Forbes, P., Chen, Z.A. and Ruth, D.W., 1994b, Quantitative analysis of radial effects on centrifuge capillary pressure curves: *SPE unsolicited paper 28182*. also presented in The 1994 SPE Annual Technical Conference and Exhibition, New Orleans, Louisiana, Sept 24-28.

Golaz, P. and Bentsen, R.G., 1980, On the use of the centrifuge to obtain capillary pressure data: *CIM paper No.80-31-38* presented at the CIM 31st Annual Technical Meeting, Calgary, May 25-28.

Hassler, G.L. and Brunner, E., 1945, Measurement of capillary pressures in small samples: *Petroleum Transactions, AIME*, **160**, 114-123.

Hirasaki, G.J. and Rohan J.A., 1993, Recommendations for determining production data. *The Centrifuge Capillary Pressure Workshop* at The Society of Core Analysts 1993 Annual Technical Conference, Houston, Texas, August 9-11.

Klute, A, 1986, *Methods of Soil Analysis: Part I. Physical and Mineralogical Methods* (2nd Edition No.9), American Society of Agronomy, Inc..

Maron, M.J., 1982, *Numerical Analysis: A Practical Approach*, Macmillian Publishing Co., Inc., New York.

Nordtvedt, J.E. and Kolltveit, K., 1991, Capillary pressure curves from centrifuge data by use of spline functions. *SPE Reservoir Evaluation*, **6**, 497-501.

Ruth, D.W. and S. Wong, 1990, Centrifuge capillary pressure curves. *Journal of Canadian Petroleum Technology*, **29**, 67-72.

Ruth, D.W. and Chen, Z.A., 1992 (submitted), On the measurement and interpretation of centrifuge capillary pressure curves: The SCA survey data. *The Log Analyst* (accepted for publication and in press).

Stroud, A.H. and D. Secrest, 1966,*Gaussian Quadrature Formulas*, Prentice-Hall, Inc., Englewood Cliffs, New Jersey.

Thomeer, J.H.M., 1960, Introduction of a pore geometrical factor defined by the capillary pressure curves. *Petroleum Transaction, AIME*, **219**, 354-358 (1960).

Thomas, G.B., Jr., 1960, *Calculus and Analytical Geometry* (Third Edition)-Chapter 15: Multiple Integrals, Addison-Wesley Publishing Company, Inc., Reading, Massachusetts.

Yuan, H.H., 1993, Review of survey procedures and experimental results. *The Centrifuge Capillary Pressure Workshop* at The Society of Core Analysts 1993 Annual Technical Conference, Houston, Texas, August 9-11.